Thin Solid Films, *185* (1990) 347–362
CONDENSED MATTER FILM BEHAVIOUR

ON THE BREAKDOWN STATISTICS OF VERY THIN SiO_2 FILMS

J. SUÑÉ, I. PLACENCIA, N. BARNIOL, E. FARRÉS, F. MARTÍN AND X. AYMERICH
Centro Nacional de Microelectrónica-Departament de Física, Universidad Autónoma de Barcelona, 08193-Bellaterra (Spain)

(Received February 21, 1989; accepted September 6, 1989)

In accordance with the idea that the degradation of the SiO_2 network and the dielectric breakdown are intimately related, a new model to describe the breakdown statistics of thin SiO_2 films is presented. The obtained distribution of failures has been found to provide very good fits of the experimental statistical data that correspond to both constant-current and constant-voltage stress experiments. The fundamental properties of the extreme-value distributions are preserved by the presented model and, what is more important, the two involved statistical parameters have a natural physical interpretation. Finally, the Monte Carlo method has been applied to simulate the degradation of the SiO_2 film until breakdown, and this has been demonstrated to be a powerful technique for introducing second-order effects into the study of the breakdown statistics.

1. INTRODUCTION

The phenomenon of dielectric breakdown in insulating films is of great importance in semiconductor devices. When measuring the time to breakdown in static tests or the breakdown field in dynamic tests, a distribution of results is found. The dielectric breakdown is related in some way to a random mechanism.

The study of the breakdown statistics is of great interest because there is the need to increase the reliability of future very-large-scale and ultralarge-scale integration devices. Moreover, the comprehension of the breakdown statistics may help to understand the physics of the mechanism of dielectric breakdown which is still unclear.

Early theories on electronic dielectric breakdown were fundamentally based on band-to-band impact ionization (BBII) processes[1]. Although some researchers are still convinced that a positive feedback mechanism including BBII and trapping of holes near the injecting interface is responsible for the dielectric breakdown[2,3], both experimental and theoretical evidence against BBII in thin SiO_2 films has recently appeared in the literature[4–6]. Evidence against the fundamental role of positive charge generation in determining the breakdown also exists[7–13].

Nowadays, the phenomenon of dielectric breakdown is being considered as a

0040-6090/90/$3.50

two-step process[11–17]. When subjected to electrical stress, either dynamic or static, the SiO_2 network progressively degrades until a threshold degradation is reached and a new conduction mechanism produces the final effective dielectric breakdown.

The degradation is believed to consist in the generation of neutral trapping sites that become partially occupied by electrons. When a certain critical density of defects is locally reached, the breakdown conduction mechanism is triggered and, usually, destructive thermal effects open a low-resistance ohmic path between the electrodes[11,12,15–17]. The physics of the final breakdown mechanism is not yet known although several reasonable hypotheses have been proposed[18,19].

The purpose of this paper is to present a model for the breakdown statistics which is compatible with the intrinsic relation between the degradation of the SiO_2 structure and the dielectric breakdown. Such a model is presented and compared with previous results and theoretical approaches of other workers.

2. BREAKDOWN STATISTICS: STATE OF THE ART

2.1. *Experimental techniques*

The experimental study of the breakdown statistics presents several difficulties. First of all, to obtain a reliable experimental distribution, we should perform a large number of measurements (*i.e.* 10^2–10^3 breakdown events should be recorded). This fact implies that, in principle, we need a large number of samples with homogeneous characteristics to obtain reliable results. However, two breakdown modes are mixed, not only in the case of SiO_2 but also in other insulators[20,21]. If the oxide is not of high quality, or if the area is not small enough, defect-related breakdown might hide the actual statistics of intrinsic dielectric breakdown[22]. Nowadays, high quality small metal–oxide–semiconductor (MOS) capacitors can be fabricated, and the breakdown statistics can be obtained by forcing the breakdown of more than 100 capacitors[23–27]. However, to avoid the limitations imposed by the requirements of high quality and homogeneity which were not able to be achieved at that time, the elegant self-healing technique was developed[28–31]. The metal electrode has to be thin enough to be volatilized in the region of the breakdown event so as to disconnect this region from the rest of the sample. Since the area of these breakdown spots is very small (smaller than 10^{-4} of the total capacitor area), many breakdowns can be recorded without altering the capacitor substantially. The self-healing technique has been widely used in the past and it is still used at the moment with great success[21].

Even if both the use of the self-healing technique and the study of high quality small devices allow us to obtain reliable statistical data, we should be aware of two additional problems. If the time interval between measurements is not small enough, or if the number of recorded events is not high enough, the experimental distribution would show the effect of censoring which has been described by Rowland *et al.*[21] In addition, the measured distribution is a mixture of defect-related and intrinsic breakdown for all the values of the random variable (time or field) and, hence, the two components cannot always be separated[21].

When a breakdown event is recorded, it can be interesting to proceed to the examination of the final state of the capacitor. Direct images of the breakdown spots

have been obtained by means of scanning electron microscopy (SEM) and other more sophisticated techniques[22,23,32].

2.2. General features of the statistics of thin insulators

From the experimental statistical data obtained during years of investigations, several features of the breakdown statistics have already been determined.

(1) The breakdown is a local phenomenon. This conclusion can be derived from electric measurements[33,34], and from SEM images which provide direct evidence of the existence of breakdown spots[22,23]. In fact, the self-healing technique would have been impossible if the breakdown had not been local. This observation is not really a property of the breakdown statistics, but its implications as to the random nature of the degradation and breakdown are of great importance.

(2) In the extreme-value probability graphs of $\ln[-\ln\{1-F(x)\}]$ *vs.* x (x being the random variable and $F(x)$ the cumulative distribution of failures), the experimental distributions are well fitted to straight lines if the random variable is either the oxide electric field or the logarithm of the breakdown time[20–24].

(3) Two different types of breakdown have been detected: low field (or short-time) defect-related breakdown, and high field (or long-time) intrinsic breakdown[20–22]. In the extreme-value probability plots, it can be seen that the experimental distribution is composed of two straight lines with different slopes. Each line corresponds to one breakdown mechanism and the intersecting point provides information of the average density of defects[20–22].

(4) The experimental distributions are found to depend on the electrode area. In the extreme-value probability plot, the breakdown distributions corresponding to samples that only differ in their area are visualized as parallel straight lines. For the same value of the random variable, the distribution of larger capacitors is shifted $\ln(S_1/S_2)$ upwards, S_1 and S_2 being the larger and smaller areas respectively. This behaviour is unique for random processes with a weakest-link character[23,35] and justifies the use of extreme-value distributions.

(5) There is evidence which supports the idea that the breakdown mechanism is always the same independent of the type of stress. Wolters[22] demonstrated that the change from defect-related to intrinsic breakdown takes place at the same value of F independent of how the stress is performed. Other workers have demonstrated that, if a Weibull distribution is assumed to describe the breakdown statistics, the same parameters are found in static and dynamic stresses[21,24].

2.3. Evolution of the study of the breakdown statistics

Early studies on the breakdown of thin dielectric films pointed out that the breakdown field in dynamic tests and the time to breakdown in static tests were distributed, and some empirical relations between these two types of test were derived[28–31,37–40]. Some attempts to model the breakdown statistics were undertaken, but with little success in the case of SiO_2 [31].

Modern studies are centred on plotting the experimental results into extreme-value distributions[20–24,41,42]. Several forms of this type of distribution have been tried because the breakdown seems to be a process with a weakest-link character. Wolters and coworkers[20,22,23] assumed an exponential failure rate, at least when

considering the electric field as the random variable. Hill and Dissado[41,42] fitted the experimental data to a complex Weibull distribution which considers a potential form for the failure rate. Both approaches yielded excellent results, and in fact, at least in the case of wear-out data, they are absolutely equivalent.

If we assumed that the breakdown is local, that it has a weakest-link character and that the breakdown spots are independent of each other, the use of extreme-value distributions is justified. The validity of the assumption of inter-independence of the breakdown events (*i.e.* when using the self-healing technique) is not easy to establish since propagating effects have been observed[43]. In any case, the experimental results have shown that both the Weibull and the double-exponential forms of the extreme-value distributions are suitable for describing the breakdown statistics. Nevertheless, once the appropriate type of distribution function has been found, we should be able to relate the statistical parameters (*i.e.* the Weibull parameters) to the actual physics of the breakdown mechanism. Probably the more important theoretical studies have been undertaken by Hill and coworkers[21,41,42]. They provided strong support for the use of the Weibull distribution by deriving it from a model based on time-dependent local fluctuations of the oxide electric field[41]. They studied three possible breakdown mechanisms: homogeneous breakdown, tree-growth-assisted breakdown and tree growth breakdown. However, they were unable to decide from the experimental results which is the most suitable for describing the actual breakdown statistics, but they did demonstrate that, on the assumption that the breakdown is triggered when a critical electric field is locally reached, the physics of breakdown yield a Weibull distribution. Since, as pointed out above, there is evidence that the electric field is not the crucial parameter in determining the breakdown, the approach of Hill and coworkers is not the most suitable for giving a physical interpretation of the statistical parameters. In this paper, we present an alternative model which is compatible with the intrinsic relationship that exists between the breakdown and the previous degradation of the SiO_2 network. The derived statistical distribution function preserves the extreme-value character and, in addition, yields a natural interpretation for all the parameters involved.

3. THEORY

Recently, we presented a model which was based on the idea that, on the average, the so-called intrinsic breakdown was triggered by the presence of a critical average density of neutral electron traps[16,17] $\bar{\rho}_{bd}$. The evolution of stress conditions was explained by considering the partial filling of those traps, and the average breakdown density was determined from the experimental times to breakdown. Analysis of data published by different workers yielded an average density of 10^{18}–10^{19} filled traps cm^{-3} in oxides 10 nm thick. The thickness dependence of $\bar{\rho}_{bd}$ could not be derived because the physics of the final run-away process are not yet known, but that model provides a suitable framework for the study of the breakdown phenomena. The statistics of breakdown should also be explained in this framework and, hence, the local nature of breakdown should be introduced.

The distribution of breakdown times or breakdown fields is due to the lack of a

deterministic relationship between the average oxide degradation and the occurrence of breakdown. The degradation is produced somehow at random over the structure area, and the final run-away is triggered when a certain degree of degradation is locally reached. In this picture, two independent parameters are to be defined: (1) the local degradation degree that triggers the final run-away; (2) the minimum area that has to reach this degradation level for the breakdown to be effective.

To build up the distribution of breakdowns, we divide the total capacitor area S_T in N cells of area S_0. The local breakdown triggering condition is defined by assuming that a constant number n_{bd} of traps must have been generated in one of these cells. In brief, when a fixed number of defects are generated in one columnar cell defined by S_0 and t_{ox}, the breakdown current run-away mechanism is triggered.

It could be argued that there is also the possibility of assuming a local critical density of defects instead of a thickness-independent number of traps. The physics of the final run-away mechanism would determine which of the two assumptions is the most suitable. Since this final run-away mechanism has not been identified yet, there is no definitive argument to reject one of the above hypotheses and the truth probably lies somewhere between them. Nevertheless, since the breakdown seems to be controlled by defects generated near the injecting interface rather than by bulk distributed defects[26], the assumption of a constant number of defects seems more reasonable. In any case, the thickness dependence is avoided by limiting this study to MOS structures with a thickness of about 10 nm.

As a first approximation, it is assumed that the rate of generation of defects is independent of the degradation degree already reached. The cells are also assumed to be independent of each other as in the case of deriving the extreme-value distributions[23].

Under these assumptions, the probability of finding a cell with n defects when the average density of defects is $\bar{\rho} = \bar{n}/S_0 t_{ox}$, $\bar{n}$ being the average number of defects per cell, is given by the Poisson distribution law if N is not too small. Since N is always of the order of 10^6–10^7,

$$P(n,\bar{\rho}) = \frac{(\bar{\rho} S_0 t_{ox})^n \exp(-\bar{\rho} S_0 t_{ox})}{n!} \tag{1}$$

where $P(n,\bar{\rho})$ is the above defined probability of finding n defects in one cell. One cell breaks down when n reaches n_{bd}. Hence, the probability that a cell has broken down is

$$P_{bd}(\bar{\rho}) = 1 - \sum_{n=0}^{n_{bd}-1} \frac{(\bar{\rho} S_0 t_{ox})^n \exp(-\bar{\rho} S_0 t_{ox})}{n!} \tag{2}$$

In such conditions, the probability of survival of an MOS structure of area $S_T = NS_0$ is

$$V(\bar{\rho}) = \{1 - P_{bd}(\bar{\rho})\}^N \tag{3}$$

and, hence, the cumulative distribution of failures should be given by

$$F(\bar{\rho}) = 1 - \left\{ \sum_{n=0}^{n_{bd}-1} \frac{(\bar{\rho} S_0 t_{ox})^n \exp(-\bar{\rho} S_0 t_{ox})}{n!} \right\}^N \tag{4}$$

This distribution function only depends on two parameters, S_0 and n_{bd}, which are naturally related to the breakdown physics. If we take $\ln(\bar{\rho})$ as the random variable and calculate $\ln[-\ln\{1-F(\bar{\rho})\}]$, the distribution given by eqn. (4) appears to be some sort of extreme-value distribution:

$$\ln[-\ln\{1-F(\bar{\rho})\}] = \ln S_1 + \ln\left[\bar{\rho}t_{ox} - \frac{1}{S_0}\ln\left\{\sum_{n=0}^{n_{bd}}\frac{1}{n!}(S_0 t_{ox}\bar{\rho})^n\right\}\right] \tag{5}$$

Since S_0 and n_{bd} might only depend on the oxide quality and on t_{ox}, the dependence of $F(\bar{\rho})$ on the structure area is entirely given by the term $\ln S_1$. The experimental data support this kind of area effect which is the same as that found in extreme-value distributions.

The fundamental problem of relating the degradation and the breakdown statistics is already solved, but eqn. (4) cannot be directly compared with the experimental results. To determine whether the experimental data can be fitted to this equation, the relation between $\bar{\rho}$ and the stress time should be investigated. The functional dependence $\bar{\rho} = \bar{\rho}(t)$ is different for each kind of stress and was determined in previous work where the average relation between degradation and breakdown was established[16,17]. In the case of a constant-current stress, this relation was found to be

$$\bar{\rho}(t) = \bar{\rho}(0) + \frac{2\varepsilon_{ox}V_{in}}{qt_{ox}^2}\left\{\exp\left(\frac{t}{\tau_V}\right) - 1\right\} \tag{6}$$

where ε_{ox} is the oxide permittivity, $\bar{\rho}(0)$ the initial density of neutral traps, V_{in} the initially applied voltage needed to obtain the desired constant current level, q the electronic charge, t_{ox} the oxide thickness and τ_V the characteristic time of evolution of the voltage which is due to the generation of the new electron traps. Since $\tau_V \gg t_{bd}$, $\exp(t/\tau_V) \approx 1 + t/\tau_V$ and eqn. (6) becomes a straight line. There is experimental evidence of a linear evolution of the applied voltage in constant-current stresses[15,44]. In the case of a constant-voltage stress, $\bar{\rho}(t)$ is given by

$$\bar{\rho}(t) = \bar{\rho}(0) + \frac{2\varepsilon_{ox}F_0^2}{K_2 t_{ox} q}\left\{\frac{\ln(1+t/\tau_J)}{1+(F_0/K_2)\ln(1+t/\tau_J)}\right\} \tag{7}$$

where F_0 is the constant applied electric field, K_2 the exponential parameter of the Fowler–Nordheim current expression and τ_J the characteristic time of evolution of the current density in this kind of tests. The relation $\tau_J = \tau_V(F_0)F_0/K_2$ between τ_J and τ_V was established[16]. The case of ramped-voltage or ramped-current tests are not discussed here because they require numerical methods to obtain the $\bar{\rho} = \bar{\rho}(t)$ relationship.

4. COMPARISON WITH PUBLISHED EXPERIMENTAL DATA

On substitution of eqns. (6) and (7) into eqn. (4), depending on the type of the test to be studied, the time-dependent distribution is found. In both cases it seems that we introduce two independent additional parameters, $\bar{\rho}(0)$ and τ_V (or τ_J). However, they are not actually new statistical parameters. As shown in ref. 16, τ_V and $\bar{\rho}(0)$ can be determined from the $V = V(t)$ characteristic under constant-current

conditions of only one sample, since all the structures of one set follow the same curve independently of their breakdown time[15,27,44]. The value of τ_V is easily determined from the slope of the $V(t)$ curve while $\bar{\rho}$ is more difficult to obtain because of the initial trapping–detrapping transients. For simplicity, in this work we have assumed that $\bar{\rho}(0) = 0$ for all the analysed samples. In brief, $\bar{\rho}(0)$ and τ_V (or τ_J) are not true statistical parameters and ought to be determined from the evolution of the stress conditions. For this reason, to analyse published data, we need to choose those studies that provide both the experimental statistics of breakdown and the evolution of the stress conditions. For the case of constant-current tests we have found several papers that fit these requirements[25–27], but only one of them also presents breakdown data of constant-voltage stresses[25].

In Table I, the characteristics of the analysed samples and the derived S_0 and n_{bd} values are shown for the case of constant-current stresses, and in Table II those corresponding to constant-voltage stress experiments. To obtain the appropriate parameters that fit the experimental results, we try different n_{bd} values and calculate S_0 by successive computer iterations until the obtained mean time t_{bd} to breakdown corresponds to the experimental value.

In Fig. 1 we have plotted the experimental distributions obtained by applying

TABLE I

CHARACTERISTICS OF THE ANALYSED CONSTANT-CURRENT STRESSES AND THEIR CORRESPONDING BREAKDOWN PARAMETERS

Set	*Number*	J ($A\,cm^{-2}$)	τ_V (s)	t_{bd} (s)	n_{bd}	S_0 (cm^2)	S (cm^2)	N
1 (ref. 25)	1	0.8	186	20	14	2.5×10^{-13}	10^{-4}	4.0×10^{8}
1 (ref. 25)	2	0.6	248	49	14	1.4×10^{-13}	10^{-4}	7.1×10^{8}
1 (ref 25)	3	0.4	372	76	14	1.3×10^{-13}	10^{-4}	7.7×10^{8}
2 (ref. 26)	1	1.0	303	21	8	1.4×10^{-13}	6.4×10^{-6}	4.5×10^{7}
2 (ref. 26)	2	0.1	3030	245	8	1.3×10^{-13}	6.4×10^{-6}	4.9×10^{7}
3 (ref. 27)	1	0.5	808	30	15	8.7×10^{-13}	2.5×10^{-3}	2.8×10^{9}
3 (ref. 27)	2	0.5	808	39.5	15	8.6×10^{-13}	5.8×10^{-5}	6.7×10^{7}

All the samples of each set have been fabricated under identical conditions. The oxide thickness is of the order of 10 nm for all the samples.

TABLE II

CHARACTERISTICS OF THE ANALYSED CONSTANT-VOLTAGE STRESSES AND THEIR CORRESPONDING BREAKDOWN PARAMETERS

F_0 ($MV\,cm^{-1}$)	$J(F_0)$ ($A\,cm^{-2}$)	$\tau_V(F_0)$ (s)	t_{bd} (s)	n_{bd}	S_0 (cm^2)	S (cm^2)	$N = S/S_0$
13.75	0.55	271.3	88	7	0.47×10^{-13}	10^{-4}	2.8×10^{6}
14.0	0.81	184.3	40	7	0.54×10^{-13}	10^{-4}	2.3×10^{6}
14.25	1.17	126.8	18	7	0.64×10^{-13}	10^{-4}	2.0×10^{6}

The analysed samples are of the same type as set 1 in Table I. The oxide thickness is 11 nm.

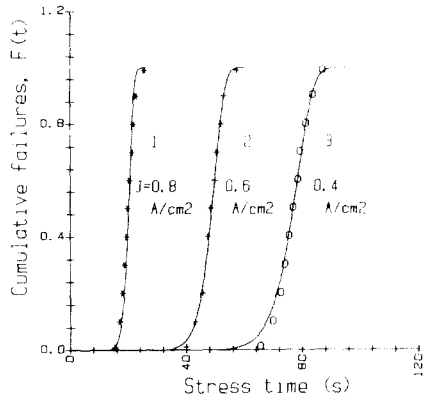

Fig. 1. Breakdown cumulative distributions for three different stressing current densities: ●, data points taken from ref. 25; — —, best fit obtained by the procedure explained in the text.

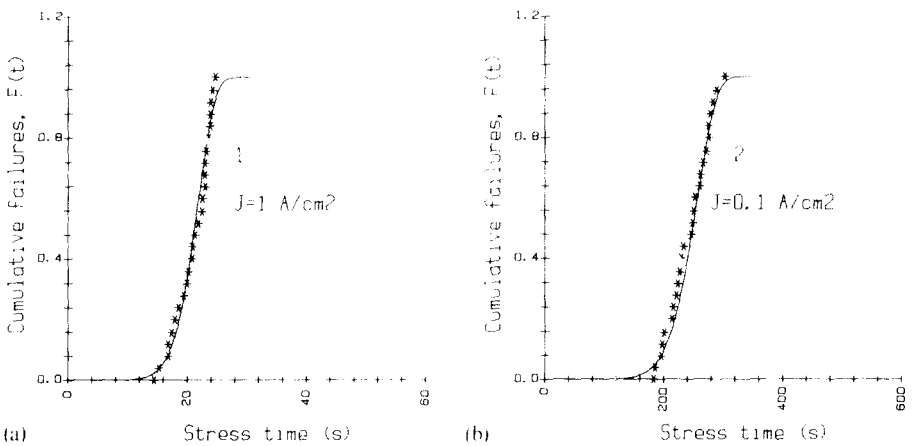

Fig. 2. Breakdown cumulative distributions for two different stressing current densities: ●, data points taken from ref. 26; — —, best fit obtained by the procedure explained in the text.

three different current levels to the same type of sample. It should be noted from Table I that n_{bd} is the same for each stress and that only a small dispersion is found in S_0 (this parameter is varied continuously while n_{bd} increases discretely, *i.e.* defect by defect). Again in Fig. 2, two different constant-current stresses are examined. It should be noted in Table I that, again, the values of n_{bd} are identical and the dispersion in S_0 is very small. However, n_{bd} is different from that obtained for the samples of set 1. In Fig. 3, we have examined the statistics of two structures of different areas subjected to the same current stress. Apart from the defect-related short-time shoulder that appears in the smaller capacitor, the fact that with almost the same values of the parameters we can fit the statistics of both samples shows that the experimental area effect is explained well by the presented model. The same data together with the theoretical fits are shown in Fig. 4 in an extreme-value probability

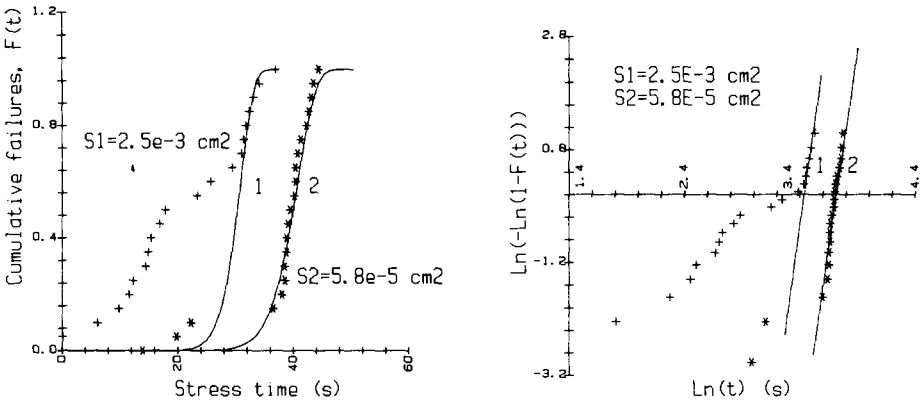

Fig. 3. Breakdown cumulative distributions for two samples of different areas subjected to 0.5 A cm^{-2}: ●, data points taken from ref. 27; ——, best fit obtained by the procedure explained in the text and only considering the intrinsic breakdown region. The short-time shoulder of sample 1 is due to defect-related breakdown.

Fig. 4. Extreme-value probability plot of the data shown in Fig. 3.

plot. This figure clearly demonstrates that the distribution proposed in eqn. (4) is compatible with an extreme-value distribution. In the intrinsic breakdown region, the plot is a straight line in both cases. Both lines seem to be parallel in this scale (closer examination of this intrinsic breakdown region shows that they are not strictly parallel), and the shift is $\ln(S_1/S_2)$. The shoulder observed in the short-time region of sample 1 can also be fitted to a straight line, and from the intersecting point the defect density of these samples can be obtained[22,23]. As pointed out above, this shoulder is due to defect-related breakdown.

In Fig. 5 we have plotted on an extreme-value probability plot the statistics of MOS capacitors subjected to different constant-voltage stresses. The values of τ_J have been derived from the τ_V values obtained by subjecting the same samples to constant-current stress conditions. From Table II we note that the dispersion of the statistical parameters used to fit these three cases is very small. The plots predicted by substituting eqn. (7) into eqn. (4) are not actually straight lines, but the experimental data also show almost the same curvature. Those fits provide further support to the presented model.

5. DISCUSSION

In the previous section we have demonstrated that the derived distribution of failures preserves the properties of extreme-value statistics, From Table I we can see that the values of n_{bd} and S_0 are almost independent of the stress current for each set of samples. However, both parameters vary slightly from one set to another. This variation could be due to the presence of different levels of initial degradation that have been ignored by assuming that $\bar{\rho}(0) = 0$ for all the samples. The samples whose constant-voltage stress characteristics are shown in Table II are the same that were analysed as set 1 in Table I. In this case, the different values of the parameters cannot

be attributed to different fabrication conditions. However, these differences in the statistical parameters, which correspond to the same samples stressed under both constant-voltage and constant-current conditions throw more doubt on the actual validity of eqns. (6) and (7) and on the relation between τ_V and τ_J than on the presented statistical model. The most interesting result that can be derived from the parameter fitting is that S_0 is always of the same order of magnitude independent of the type of stress and fabrication conditions, *i.e.* ($0.36-8.7\times10^{-13}$ cm^2 for the analysed samples). This value of S_0 is much smaller than the area of the breakdown spots observed after self-healing events which are of 2–5 μm in diameter[22,23]. However, the obtained S_0 value is in accordance with the estimated area of the spots of high leakage conduction found by other workers[33] before the breakdown event. Evidently, the physical interpretation of S_0 is much closer to the area of the prebreakdown degraded spots than to one of the breakdown spots where important thermal effects have taken place.

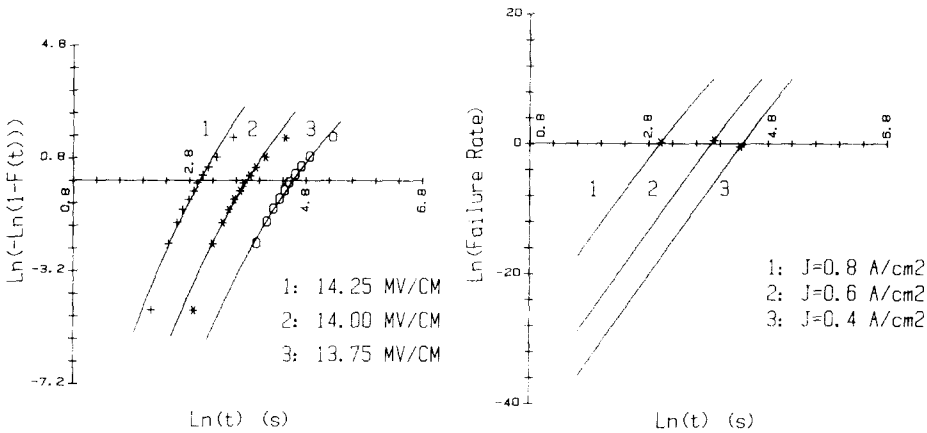

Fig. 5. Breakdown cumulative distributions in an extreme-value probability plot obtained when subjecting the samples to three different constant-voltage stresses: data points are taken from ref. 25, the samples are the same as those in Fig. 1; ——, best fit obtained by the procedure explained in the text.

Fig. 6. Failure rate function as a function of stress time for three different constant-current stresses: ✳, experimental mean times to breakdown. The samples are those in Fig. 1, and the parameters S_0 and n_{bd} are those of set 1 in Table I.

The equivalence between the presented model and the extreme-value statistics has been demonstrated, and we have shown that S_0 and n_{bd} are suitable parameters with a simple and natural physical interpretation. However, several details of the experimental breakdown statistics need further discussion. When studying the reliability of simple systems, as in the case of breakdown of single MOS capacitors, the function that provides direct physical information about the type of mechanism that causes the failure of the elements under study is the failure rate. The failure rate, also known as the force of mortality or the Mills ratio, is the probability of failure at a determined value of the random variable knowing that the element has survived so

far. As we know that the failure rate is given by

$$a(t) = -\frac{\mathrm{d}}{\mathrm{d}t}[\ln\{V(t)\}] \tag{8}$$

eqns. (2) and (3) yield

$$a(t) = \left[S_T t_{ox}(\bar{\rho} S_0 t_{ox})^{n_{bd}-1} \Big/ \left\{(n_{bd}-1)! \sum_{n=0}^{n_{bd}-1} \frac{(\bar{\rho} S_0 t_{ox})^n}{n!}\right\}\right]\left(\frac{\mathrm{d}\bar{\rho}}{\mathrm{d}t}\right) \tag{9}$$

after straightforward calculations. Of course, the time-derivative of the average density of defects depends on the type of test and should be calculated from eqns. (6) and (7) in the case of static tests. In Figs. 6 and 7, the failure rate is depicted for three constant-current stress experiments (set 1 in Table I), and for three constant-voltage stresses (Table II). The values of S_0 and n_{bd} are those of Tables I and II, and the asterisks indicate in each case the experimental mean time to breakdown. In both figures the failure rate increases with increasing time, although in the case of constant-voltage tests it tends towards saturation. This increase in the failure rate is a direct indication of the relation that exists between the breakdown and the degradation of the SiO_2 structure. A decreasing failure rate indicates that the process is related to defects, a time-independent failure rate corresponds to random failures, and, if $a(t)$ increases with increasing time, there must be an aging process involving some degradation of the structures. In the case of extreme-value distributions, the slope of the cumulative distribution of failures of the extreme-value probability plot directly indicates how the failure rate changes with time. In principle, as pointed out elsewhere[21,24,42], if the slope is smaller than unity, the breakdown is defect related and, if it is greater than unity, the breakdown is related to a degrading process. In Table III we review the values of the slopes of the extreme-value probability plots of experimental breakdown distributions found by different workers[24–26,44]. In the case of ramped voltage measurements, the value of the slope

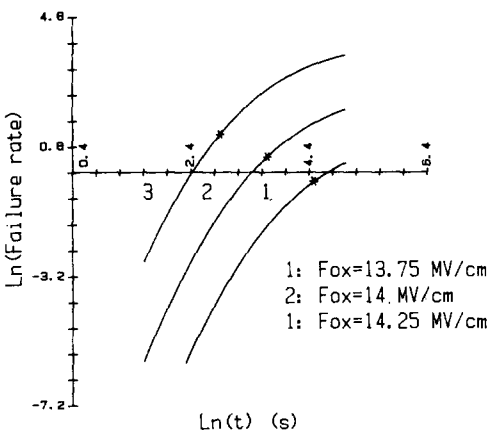

Fig. 7. Failure rate function as a function of stress time for three different constant-voltage stresses: ✳, experimental mean times to breakdown. The samples are those in Fig. 5, and the parameters S_0 and n_{bd} are those in Table II.

does not correspond to the actual experimental slope, but to one of the Weibull parameters determined from the experimental distribution that, at this time, corresponds to the slope that would have the breakdown distribution if the structure had been subjected to a constant-voltage stress[24,42]. Many of the values in Table III have not been taken directly from the indicated source work, but from the paper of Hill and Dissado[42] who presented a very complete review of the breakdown of thin insulators.

TABLE III

SLOPE OF THE INTRINSIC BREAKDOWN DISTRIBUTION IN THE EXTREME-VALUE PROBABILITY PLOT UNDER DIFFERENT STRESS CONDITIONS

Type of stress	*Slope*	*Reference*
Constant (ramped measurements) voltage	0.58	Ref. 45
	0.34	Ref. 24
Constant (constant measurements) voltage	0.24	Ref. 24
	2.5	Ref. 25
Constant current	12	Ref. 25
Constant current	7.5	Ref. 26
Constant current	4.2	Ref. 44

In the case of ramped measurements, the value of the slope is not the experimental value, but the value of one of the Weibull parameters which corresponds to the slope that would be found in constant-voltage tests.

For constant-current experiments, the slope of the extreme-value probability plot is always greater than unity, but this is not the case for constant-voltage stresses. A fundamental question about the nature of the intrinsic dielectric breakdown arises: is the so-called intrinsic breakdown a defect-related process? The statistical data do not provide enough information to answer this question. However, the evolution of the stress conditions in wear-out tests clearly indicates that the oxide structure becomes more and more degraded as the stress time increases, and that the breakdown is intimately related to this degradation. The degradation of the SiO_2 network is reflected in the generation of electron traps that become partially filled because of the dynamic equilibrium between trapping and detrapping mechanisms. The generation of a negative charge in the oxide causes a positive feedback process in constant-current experiments and a negative feedback process in constant-voltage stresses. It is easy to show that positive feedback enhances the actual slope of the extreme-value probability plot while negative feedback reduces it. In Fig. 7 we can see that, owing to this negative feedback process, the failure rate tends to saturate in the case of constant-voltage stresses. In brief, the effects of negative charge trapping can explain the dependence of the slope of the extreme-value probability plot on the type of stress. A clear indication of these effects is seen in Fig. 4 where even the slope of the usually considered defect-related breakdown region of the cumulative distribution is greater than unity. This is due to the positive feedback mechanism that occurs during constant-current tests.

Let us now examine the area effect in detail. If the defect-related shoulder

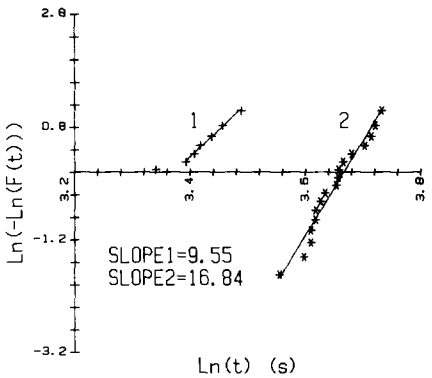

Fig. 8. Enhanced extreme-value probability plot corresponding to the data shown in Figs. 3 and 4. Each line corresponds to two groups of capacitors of the same type which differ in their area.

obtained in the breakdown distribution of smaller capacitors is omitted, the scale of the $\ln(t)$ axis is increased and more details can be observed. This has been done in Fig. 8 where it can be seen that the distribution lines are not actually parallel as predicted by the extreme-value statistical model. Several causes can be responsible for this effect.

(1) There is a mixture of breakdown mechanisms related to the presence of defects in the as-fabricated oxide[21].

(2) There are different influences of the censoring of the experimental data[21] in structures of different areas. The censoring due to the limited number of recorded breakdown events has a more important influence on small-area capacitors, while the time resolution censoring changes the distribution of large-area devices rather than those of the smaller devices.

(3) The fundamental hypothesis of the extreme-value model fails because (a) the cells are not independent (*i.e.* there are propagating effects) on (b) the rate of failure is a local property that depends on the local degradation of the oxide.

Items (1) and (2) have been extensively studied by Rowland *et al.*[21] and fundamentally depend on the experimental set-up. The study of (3) is much more complicated and cannot be treated by assuming the validity of the extreme-value distribution. The presented model suggests a natural way of introducing these second-order effects. However, to introduce these effects, the analytical treatment have to be abandoned and the problem has to be faced with Monte Carlo simulation methods.

The distribution given by eqn. (4) can also be obtained by simulating the degradation process by means of the Monte Carlo technique. The structure area is divided into N cells, and defects are generated at random over these cells until the number of defects of one cell reaches n_{bd} which is the breakdown triggering condition. The procedure is repeated for many capacitors, and the distribution given by eqn. (4) is found if the probability of growth of defects is the same for all the cells. This kind of simulation allows us to introduce easily the dependence of the degradation rate on the cell degradation degree already reached and to compare the results with those obtained by means of eqn. (4). However, several important

problems are to be faced. First of all, there is the requirement of working with reasonable short computer times. Hence, it is almost impossible to simulate the breakdown of even very-small-area capacitors because of the always large number of cells (see Tables I and II). A reasonable number of cells (10^3–10^4) has to be chosen to undertake a simulated study of the dielectric breakdown statistics under different stress conditions. However, the logarithmic area effect cannot be used to predict the breakdown of greater structures because the non-constant degradation rate might cause the area dependence to change. In spite of these limitations, the Monte Carlo method can be used to introduce the local degradation feedback dependence and to compare the obtained results with the distribution given by eqn. (4) which assumes a homogeneous failure rate.

Since there is no definitive experimental evidence to support or refuse a positive (enhancement of the degradation rate with the growth of the degradation degree) or a negative (reduction in the degradation rate with the growth of the degradation degree) feedback mechanism, we have carried out several simulations considering a different mechanism in each case. In Fig. 9, the simulated cumulative distributions are plotted in an extreme-value probability graph. In all the cases, the plots obtained are almost straight lines, even if the effects of censoring are clearly seen in the initial curvature of each distribution. Thus the breakdown statistics yielded by this modified model are still compatible with extreme-value distributions, but the values of the parameters S_0 and n_{bd} might change because of the effects of the feedback mechanisms. As expected, the time to breakdown is shorter if the feedback is positive and longer if it is negative. No clear area dependence of the slope of the extreme-value distribution plot has been found. Stronger feedback processes may show a more defined area dependence.

Even if the simulations have not yielded for the moment very new results, we wish to emphasize that this can be a very powerful technique to introduce second-order effects in the study of the breakdown statistics. On the contrary, it would be

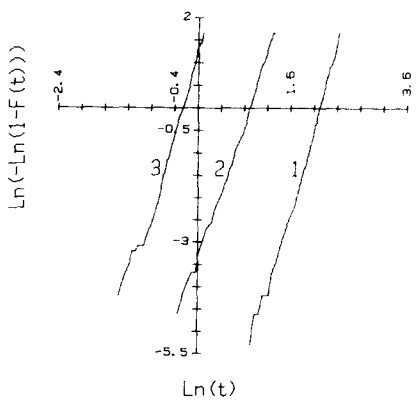

Fig. 9. Extreme-value distribution plots obtained by Monte Carlo simulations. ($n_{bd} = 5$; $S_0 = 5 \times 10^{-13}$ cm^2; $N = 25\,600$; $F = 14$ MV cm^{-1}; $t_{ox} = 10$ nm): curve 1, negative feedback mechanism, the local current decreases with the cell degradation; curve 2, Poisson distribution; curve 3, positive feedback mechanism, the local current increases with increasing cell degradation.

very difficult to introduce these effects if we assume a fixed functional dependence for the distribution of breakdowns (*i.e.* Weibull or double-exponential distributions).

6. CONCLUSIONS

On the assumption that the dielectric breakdown is the final consequence of the degradation of the SiO_2 network, a new model to describe the breakdown statistics of thin SiO_2 films has been presented. The obtained distributions of failures preserve the main properties of extreme-value statistics, and they depend on two parameters which have a simple and natural physical meaning. In agreement with recently published results, the area of the degraded spots that trigger the final run-away breakdown mechanism has been found to be of the order of 10^{-13} cm^2. Several second-order effects have also been discussed, and Monte Carlo simulations have been proposed as an alternative powerful technique for the theoretical study of the breakdown statistics.

ACKNOWLEDGMENT

This work was partially supported by the Comisión Interministerial de Ciencia y Tecnología.

REFERENCES

1 N. Klein, *Thin Solid Films, 50* (1978) 223.
2 I.-C. Chen, S. E. Holland and C. Hu, *IEEE Trans. Electron Devices, 32* (1985) 413.
3 J. C. Lee, I.-C. Chen and C. Hu, *IEEE Trans. Electron Devices, 35* (1988) 2268.
4 Z. A. Weinberg, M. V. Fischetti and Y. Nissan-Cohen, *J. Appl. Phys., 59* (1986) 824.
5 D. J. DiMaria and M. V. Fischetti, *Appl. Surf. Sci., 30* (1987) 278.
6 W. L. Warren and P. M. Lenahan, *J. Appl. Phys., 62* (1987) 4305.
7 S. Haddad and S. M. Liang, *IEEE Electron Devices Lett., 8* (1987) 524.
8 M. Dutoit, P. Fazan, A. Benjelloun, M. Ilegems and J. M. Moret, *Appl. Surf. Sci., 30* (1987) 333.
9 Y. Nissan-Cohen and T. Gorczyca, *IEEE Electron Devices Lett., 9* (1988) 287.
10 Y. Nissan-Cohen, J. Shappir and D. Frohman-Bentchkowsky, *J. Appl. Phys., 58* (1985) 2252.
11 E. Avni and J. Shappir, *J. Appl. Phys., 64* (1988) 743.
12 Z. A. Weinberg and T. N. Nguyen, *J. Appl. Phys., 61* (1987) 1947.
13 Y. Nissan-Cohen, J. Shappir and D. Frohman-Bentchkowsky, *J. Appl. Phys., 60* (1986) 2024.
14 D. R. Wolters and A. T. A. Zegers-van Duynhoven, *Extended Abstracts, Electrochemical Society, Spring Meet., 1987*, Electrochemical Society, Pennington, NJ, 1987, p. 226.
15 B. Balland, C. Plossu and S. Bardy, *Thin Solid Films, 148* (1987) 149.
16 J. Suñé, I. Placencia, N. Barniol, E. Farrés and X. Aymerich, *Phys. Status Solidi A, 111* (1989) 675.
17 I. Placencia, J. Suñé, N. Barniol, E. Farrés and X. Aymerich, *Proc. 18th Eur. Solid State Device Research Conf.*, in *J. Phys. (Paris), Colloq. C4, 49* (1988) 783.
18 B. Riccó, M. Ya Azbel and M. H. Brodsky, *Phys. Rev. Lett., 51* (1983) 1795.
19 B. Neri, P. Olivo and B. Riccó, *Appl. Phys. Lett., 51* (1987) 2167.
20 D. R. Wolters and J. J. van der Schoot, *Philips J. Res., 40* (1985) 115.
21 S. M. Rowland, R. M. Hill and L. A. Dissado, *J. Phys. C, 19* (1986) 6263.
22 D. R. Wolters, *Philips Tech. Rev., 43* (1987) 330.
23 D. R. Wolters and J. F. Verwey, in G. Barbottin and A. Vapaille (eds.), *Instabilities in Silicon Devices*, North-Holland, Amsterdam, 1986, p. 315.
24 S. K. Haywood, M. M. Heyns and R. F. De Keersmaecker, *Appl. Surf. Sci., 30* (1987) 325.

25 C. F. Chen, C. Y. Wu, M. K..Lee and C. N. Chen, *IEEE Trans. Electron Devices, 34* (1987) 1540.
26 P. Olivo, B. Riccó, T. N. Nguyen, T. S. Kuan and S. J. Jeng, *Appl. Phys. Lett., 51* (1987) 2245.
27 P. Olivo, T. N. Nguyen and B. Riccó, *Proc. 1st Int. Conf. on the Physics and Technology of a-SiO$_2$*, Plenum, New York, 1988, p. 449.
28 G. Siddall, *Vacuum, 9* (1960) 274.
29 N. Kein, *IEEE Trans. Electron Devices, 13* (1966) 788.
30 N. Klein, *Adv. Phys., 21* (1972) 605.
31 P. Solomon, N. Klein and M. Albert, *Thin Solid Films, 35* (1976) 21.
32 D. M. Taylor, *Proc. Inst. Electr. Eng., Part A, 128* (1981) 174.
33 T. N. Nguyen, P. Olivo and B. Riccó, *Proc. International Reliability Physics Symp.*, IEEE New York, 1987, p. 66.
34 P. A. Heinmann, *IEEE Trans. Electron Devices, 30* (1983) 1366.
35 M. Shatzkes and M. Av.-Ron, *Thin Solid Films, 91* (1982) 217.
36 G. Ghidini and A. Modelli, in J. J. Simonne and J. Buxó (eds.), *Insulating Films on Semiconductors*, North-Holland, Amsterdam, 1986, p. 141.
37 C. M. Osburn and D. W. Ormond, *J. Electrochem Soc., 119* (1972) 597.
38 C. M. Osburn and E. Bassous, *J. Electrochem. Soc., 122* (1975) 89.
39 D. L. Crook, *1978 Int. Electron Devices Meet.*, Dig. Tech. Papers, IEEE, New York, 1978, p. 444.
40 A. Berman, *Proc. Int. Reliability Physics Symp.*, IEEE, New York, 1981, p. 208.
41 R. M. Hill and L. A. Dissado, *J. Phys. C, 16* (1983) 2145.
42 R. M. Hill and L. A. Dissado, *J. Phys. C, 16* (1983) 4447.
43 N. Klein and H. Gafni, *IEEE Trans. Electron Devices, 13* (1966) 281.
44 E. Harari, *J. Appl. Phys., 49* (1978) 2478.
45 M. Shatzkes and M. Av.-Ron, *IBM J. Res. Dev., 25* (1981) 167.